

Constraints on Models for Proton-Proton Scattering from Multi-strange Baryon Data

F.M. Liu^{1,2}, J. Aichelin¹, M. Bleicher¹, H.J. Drescher³, S. Ostapchenko^{4,5}, T. Pierog¹, and K. Werner¹

¹ SUBATECH, Université de Nantes – IN2P3/CNRS – Ecole des Mines, Nantes, France

² Institute of Particle Physics, Huazhong Normal University, Wuhan, China

³ Physics Department, New York University, New York, USA

⁴ Institut für Experimentelle Kernphysik, University of Karlsruhe, 76021 Karlsruhe, Germany

⁵ Moscow State University, Institute of Nuclear Physics, Moscow, Russia

28th December 2018

The recent data on pp collisions at 158 GeV provide severe constraints on string models: These measurements allow for the first time to determine how color strings are formed in ultrarelativistic proton-proton collisions.

Recently, the NA49 collaboration has published [1] the rapidity spectra of p , Λ , Ξ as well as the corresponding antibaryons in pp interactions at 158 GeV lab. energy. These measurements provide new insight into the string formation process. In the string picture, high energy proton-proton collisions create “excitations” in form of strings, being one dimensional objects which decay into hadrons according to longitudinal phase space. This framework is well confirmed in low energy electron-positron annihilation [2] where the virtual photon decays into a quark-antiquark string which breaks up into mesons(M), baryons(B) and antibaryons(\bar{B}). An example of a $q - \bar{q}$ string fragmenting into hadrons is shown in Fig. 1. Proton-proton collisions are more complicated in the sense that they lead, in general, to creation and hadronization of a number of strings. Besides that, the very mechanism of string formation is unclear in that case, as will be discussed in the following.

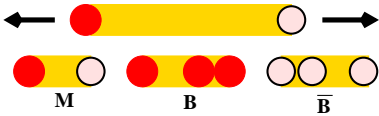


Figure 1: $e^+e^- \rightarrow \gamma^* \rightarrow q\bar{q}$. The $q - \bar{q}$ string fragments into hadrons.

One may distinguish two classes of string models:

- Longitudinal excitation (LE) models: UrQMD [3], HIJING [4], PYTHIA [5], FRITIOF [6], RQMD [7], HSD [8];
- Color exchange (CE) models: DPM [9], VENUS [2], QGS [10].

In the LE case the two colliding protons excite each other via a large transfer of momentum between projectile and

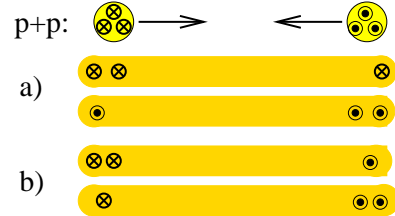


Figure 2: Two classes of string models for pp collisions: a) longitudinal excitation (LE). b) color exchange (CE).

target, Fig. 2a. In contrast, the CE picture considers a color exchange between the incoming protons, leaving behind two octet states. Thus, a diquark from the projectile and a quark from the target, and vice versa, form color singlets, which are finally identified with strings, c.f. Fig. 2b. Contrary to the LE scenario, the color exchange is a soft process, characterized by a negligible momentum transfer. The final result, two quark-diquark strings with valence quarks being their ends, however, is quite similar.

How are baryons and antibaryons produced? The easiest way to obtain baryons is to break the strings via quark-antiquark pair production close to the valence diquark. Since the incoming proton was composed of light quarks (qqq), the resulting baryon is of qqq or qqs type. Thus nucleons, Λ s or Σ s are formed. Since these baryons are produced at the string ends, they occur mainly close to the projectile rapidity or target rapidity (leading baryons).

Multi-strange baryons which consist of two or three strange quarks are produced near the quark end or the middle of the strings, via $ss\bar{s}\bar{s}$ production. Therefore the distributions of multi-strange baryons are peaked around central rapidity. Thus, the corresponding yields of multi-strange baryons and their antiparticles should be comparable. This contradicts experimental observations: The

oretically one finds the ratio of yields [11]:

$$\Xi^+/\Xi^- = 0.8 \sim 1.2.$$

Experimentally, however, Ξ^+ s are less frequent than expected. The ratio at midrapidity is [1]

$$\Xi^+/\Xi^- = 0.44 \pm 0.08.$$

The situation for Ω s is even more extreme: from string models one gets [11]

$$\Omega^+/\Omega^- = 1.6 \sim 1.9$$

at midrapidity. From extrapolating Λ and Ξ results (and from preliminary NA49 data) we expect [1]

$$\Omega^+/\Omega^- = 0.5 \sim 0.8.$$

It seems impossible to get the Ω^+/Ω^- ratio smaller than unity from string models. As addressed in [11], this is due to the fact that the strings have typically a light quark (but not a strange quark) at the end, which disfavours multi-strange baryon production.

So is there something fundamentally wrong with string models? To answer this question we consider a new approach called Parton-Based Gribov-Regge theory, realised in the Monte Carlo program NEXUS 3 [12]. Hadron-hadron interactions are treated there within an effective multiple scattering scheme, using Reggeon formalism [13]. Elementary scattering processes, happening in parallel, correspond to underlying (in general, nonperturbative) parton cascades and are described phenomenologically as Pomeron exchanges. Here one distinguishes the "soft" Pomeron, corresponding to the case of parton virtualities Q_i^2 in the cascade being all below some cut-off value Q_0^2 for pQCD being applicable, and the "semi-hard Pomeron" - representing the picture when at least a part of that cascade develops in the perturbative region $Q_i^2 > Q_0^2$. The soft Pomeron may be regarded as a two-layer (cylinder-like) "soft" parton ladder, which is attached to the projectile hadron and to the target hadron via its leg partons, c.f. Fig. 3a. The latter are assumed to form color singlets, of type $q-\bar{q}$, $q-qq$ or $\bar{q}-\bar{qq}$, with the probability of $q-qq$ and $\bar{q}-\bar{qq}$ -contributions being controloed by a parameter P_{qq} . The semi-hard Pomeron is represented by a piece of the QCD parton ladder (which stays for the perturbative "hard" part of the cascade), sandwiched between two soft Pomerons (describing non-perturbative "soft preevolution") which in turn are connected in the usual way to the projectile and to the target respectively. In case the hard parton cascade starts from a valence quark on the projectile or on the target side, no soft preevolution takes place and therefore no soft Pomeron is considered on the corresponding side. At low energies the collision process is essentially a nonperturbative one and is described entirely by multiple exchanges of soft Pomerons. Nevertheless, with the energy rising,

the relative weight of the semihard contribution fastly increases and such processes completely dominate hadronic interactions at very high energies.

Applying the so-called Abramovskii-Gribov-Kancheli cutting rules [14] allows to obtain the expressions both for hadron-hadron interaction cross sections and for partial weights of particular configurations of the interaction - as contributions of certain classes of cut diagrams. Based on this, one first determines in the Monte Carlo procedure the collision configuration: i.e. the number of cut Pomerons of each type (soft, semihard, etc.) exchanged between the projectile and the target, shares the initial energy-momentum between them, and then accounts for the particle production from two kinds of sources: cut Pomerons and the decays of remnant states, formed of the projectile and target spectator partons left after Pomeron emissions, c.f. Fig. 3a.

An intuitive way to understand particle production from cut Pomerons is given by the string model [12]; each cut Pomeron is regarded as a pair of strings, c.f. Fig. 3b. Here, for the string ends of soft and semihard Pomerons we take quarks and antiquarks from the sea in a flavor-symmetric way, letting valence quarks stay in remnant states. Thus, due to the complete flavor symmetry of the string ends, baryons and antibaryons are produced from cut Pomerons in equal amounts. The only exception is given by the (semi-)hard scattering involving valence quarks, as mentioned above. Nevertheless, the role of such processes is quite negligible at SPS energies and still remains subdominant at higher energies compared to the contribution of the usual semihard scattering. Therefore, even though all types of Pomerons are included in the Monte Carlo, the flavor-asymmetric valence-type contributions can be ignored in the following discussion.

The novelty of the current work, compared to the old version of NEXUS applied in [11], is that whenever a quark or an antiquark is taken from the sea as a string end, the corresponding antiparticle is put into the remnant state to compensate the flavour. Thus, the simplest and most frequent collision configuration has two remnants and one cut Pomeron represented by two $q-\bar{q}$ strings, as shown in Fig. 4a. Besides the three valence quarks, each remnant has additionally a quark and an antiquark.

For the mass distribution of remnant states we use $P(m^2) \propto (m^2)^{-\alpha}$, $m^2 \in (m_{\min}^2, x^+ s)$, with the parameter $\alpha = 1.5$. Here s is the squared CMS energy, m_{\min} is the minimum mass of the corresponding excited hadron state, and x^+ is the remnant light-cone momentum fraction left after cut Pomeron emissions. For each remnant, according to its quark and antiquark content, the emission of mesons, antibaryons and baryons is considered until one is left with a simple $q\bar{q}$ -, $qq\bar{q}$ - or $\bar{q}qq\bar{q}$ -configuration, which is then treated as a resonance or as a string, if its mass is large enough. For example, in the case shown in Fig. 4a, first a meson consisting of the antiquark and any of the four quarks is emitted, then

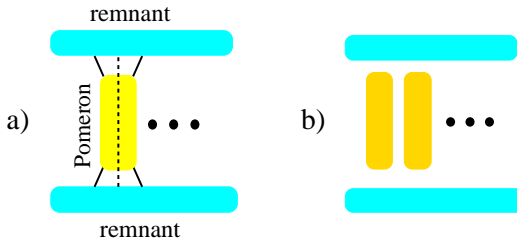


Figure 3: a) A typical collision configuration for pp collisions has two remnants and a number of Pomerons which stand for elementary interactions. Particles are produced from remnant decay and cut Pomerons. b) Each cut pomeron is regarded as two strings.

the remained part of the remnant is treated either as a baryon resonance or as a quark-diquark string. Thus, in that configuration remnant decays produce protons and Λ s which then show strong leading particle effects (two wings in the rapidity spectra), but not antibaryons or multi-strange baryons.

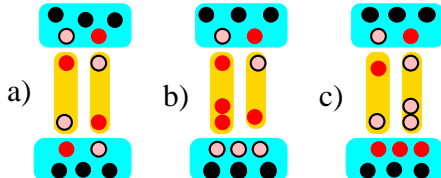


Figure 4: a) The simplest collision configuration has two remnants and one cut Pomeron represented by two $q - \bar{q}$ strings. b) One of the \bar{q} string-ends can be replaced by a qq string-end. c) With the same probability, one of the q string-ends can be replaced by a $\bar{q}\bar{q}$ string-end.

As mentioned above, a leg of a cut Pomeron may be of qqq type with some small probability P_{qq} (the mean multiplicity increases with P_{qq}), which means the corresponding string ends are a diquark and a quark. The qqq Pomeron leg has to be compensated by the three corresponding antiquarks in the remnant, as shown in Fig. 4b. The $(3q3\bar{q})$ remnant may decay into three mesons (3M) or a baryon and an antibaryon ($B + \bar{B}$). Since the 3M mode is favored by phase space, we neglect $B + \bar{B}$ production here. For symmetry reasons, the leg of a cut Pomeron may be of $\bar{q}\bar{q}\bar{q}$ type with the same probability P_{qq} . This yields a $\bar{q} - \bar{q}\bar{q}$ string and a (6q) remnant, as shown in Fig. 4c. The (6q) remnant decays into two baryons. Since q - qq strings and $\bar{q} - \bar{q}\bar{q}$ strings have the same probability to appear, baryons and antibaryons are produced equally from cut Pomerons. However, from remnant decays, baryon production is favored due to the initial valence quark content.

Fig.5 depicts the rapidity spectra of baryons and antibaryons from NEXUS 3.0 with $P_{qq} = 0.02$ and the strangeness fraction of newly produced quarks $f_s = 0.3$ (black solid lines). As a comparison, we also show the results from Pythia 6.2 simulations [5] (grey solid lines),

and the preliminary data from the NA49 experiment [1] (points). In NEXUS 3.0, particles are produced by two sources: remnants (dotted lines) and cut Pomerons (dashed lines). Fig.5 demonstrates that NEXUS 3.0 describes reasonably the rapidity spectra of baryons and antibaryons in pp collision at 158 GeV.

We also provide the particle yields at midrapidity, $y \in (y_{cm} - 0.5, y_{cm} + 0.5)$, from NEXUS 3.0, Pythia 6.2 and compare them to data in table 1.

yield	NEXUS 3.0	Pythia 6.2	NA49 data
p	1.01×10^{-1}	4.85×10^{-2}	9.28×10^{-2}
\bar{p}	2.14×10^{-2}	1.64×10^{-2}	2.05×10^{-2}
Λ	1.65×10^{-2}	7.53×10^{-3}	1.79×10^{-2}
$\bar{\Lambda}$	5.86×10^{-3}	4.02×10^{-3}	5.57×10^{-3}
Ξ^-	7.45×10^{-4}	2.53×10^{-4}	7.08×10^{-4}
Ξ^+	4.17×10^{-4}	2.20×10^{-4}	3.12×10^{-4}
Ω^-	2.68×10^{-5}	2.33×10^{-6}	—
Ω^+	1.69×10^{-5}	2.94×10^{-6}	—

Table 1: Particle yields at midrapidity in pp collisions at 158 GeV.

From NEXUS 3.0, we get the ratios at midrapidity

$$\Xi^+/\Xi^- = 0.56, \quad \Omega^+/\Omega^- = 0.71.$$

In conclusion, it seems that old string models fail to reproduce the experimental Ξ^+/Ξ^- and anticipated Ω^+/Ω^- ratio so far. The string formation mechanism as employed in NEXUS 3.0 allows to get a reasonable agreement with experimental data. One can understand the basic features of the production of multi-strange baryons as well as of Λ s and protons within the model picture of proton-proton scattering, with the corresponding final state being a system of projectile and target remnant states and in addition of a number of cut Pomerons represented by a pair of strings each. At SPS energy, the interaction dynamics is dominated by exchanges of soft Pomerons. These are vacuum excitations and produce particles and antiparticles equally, with their string ends being sea quarks. On the other hand, the valence quark content is kept into remnant states and favours leading baryon production. This explains the observed differences in the rapidity spectra of baryons and antibaryons as well as the measured baryon yields and the ratios of multi-strange baryons to their antiparticles at low energies. With the increase of the collision energy, the contribution of semihard Pomeron exchanges becomes important. Nevertheless, as discussed above, the role of valence quark hard interactions always remains subdominant. As the usual (non-valence) semihard Pomerons are connected to hadrons in exactly the same manner as the soft ones, the conclusion on the dominance of baryon over antibaryon production in the forward direction remains valid at all energies. On the other hand,

the increasing flavor-symmetric baryon-antibaryon production from string hadronization will result in the ratios of Ξ^+/Ξ^- and Ω^+/Ω^- approaching unity at very high energies.

One of the authors (SO) acknowledges support by the German Ministry for Research and Education (BMBF).

References

- [1] T. Susa *et al.*, NA49, Nucl. Phys. A698 (2002) 491c; K. Kadija, talk given at *Strange Quark Matter 2001*, Frankfurt, Germany.
- [2] K. Werner, Phys. Rept. **232** (1993) 87.
- [3] M. Bleicher *et al.*, J. Phys. G **25** (1999) 1859. [arXiv:hep-ph/9909407].
- [4] X. N. Wang, Phys. Rept. **280** (1997) 287. [arXiv:hep-ph/9605214].
- [5] T. Sjostrand *et al.*, Comput. Phys. Commun. **135** (2001) 238. [arXiv:hep-ph/0010017].
- [6] H. Pi, Comput. Phys. Commun. **71** (1992) 173.
- [7] H. Sorge, Phys. Rev. C **52** (1995) 3291.
- [8] W. Ehehalt and W. Cassing, Nucl. Phys. A **602** (1996) 449.
- [9] J. Ranft, Z. Phys. C **43** (1989) 439; A. Capella *et al.*, Phys. Rept. **236** (1994) 225.
- [10] A. B. Kaidalov *et al.*, Phys. Lett. B **117** (1982) 247.
- [11] M. Bleicher *et al.*, Phys. Rev. Lett. **88** (2002) 202501. arXiv:hep-ph/0111187.
- [12] H. J. Drescher *et al.*, Phys. Rept. **350** (2001) 93. [arXiv:hep-ph/0007198].
- [13] V. N. Gribov, Sov. Phys. JETP **26** (1968) 414.
- [14] V. A. Abramovskii, V. N. Gribov, O. V. Kancheli, Sov. J. Nucl. Phys. **18** (1974) 308.

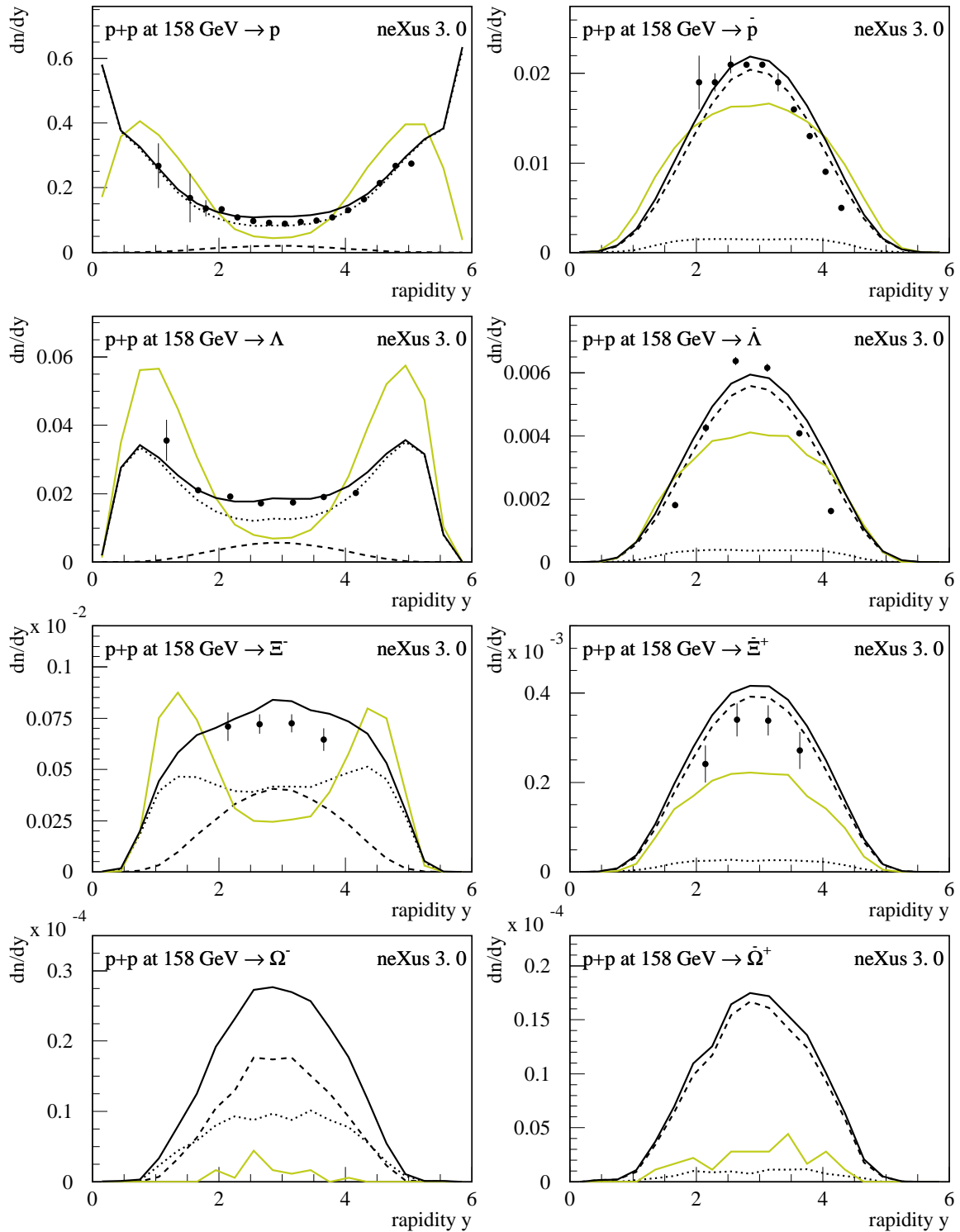


Figure 5: Rapidity spectra of baryons and antibaryons calculated from NEXUS 3.0 (remnant contribution: black dotted lines; Pomeron contribution: black dashed lines; sum: black solid lines), Pythia 6.2 (grey solid lines) and NA49 experiment [1] (points).